

An Infrared Spectroscopic and Density Functional Theoretical Investigation of the Reaction Products of Laser-Ablated Scandium and Titanium Atoms with Nitric Oxide

Gary P. Kushto, Mingfei Zhou, and Lester Andrews*

Department of Chemistry, University of Virginia, Charlottesville, Virginia 22901

Charles W. Bauschlicher Jr.*

STC-230-3, NASA Ames Research Center, Moffett Field, California 94035

Received: September 21, 1998; In Final Form: December 7, 1998

Laser-ablated Sc and Ti atoms have been reacted with NO during condensation in excess argon. Matrix infrared spectra show that the major products are the side-bonded Sc[NO] species and the inserted NScO and NTiO molecules based on isotopic substitution ($^{15}\text{N}^{16}\text{O}$ and $^{15}\text{N}^{18}\text{O}$) and DFT calculations of isotopic frequencies, which provide a match for two modes in three isotopic modifications for each molecule. The NScO and NTiO molecules are nitride/oxides with M–O stretching modes only 46–88 cm^{-1} below the diatomic metal oxides but M–N stretching modes 314–442 cm^{-1} lower than the diatomic metal nitride molecules. The ScN, ScO and TiN, TiO molecules are observed as decomposition products. Evidence is also presented for the nitrosyls ScNO and TiNO, the Sc[NO]⁺ cation, and the NTiO[−] anion.

Introduction

For decades, nitric oxide has played a role in traditional coordination chemistry.^{1,2} Along with carbon monoxide, NO has been used as a probe to study the chemistry of coordination complexes by providing a relatively simple ligand that can adopt several coordination geometries and significantly alter the electronic properties of the transition metal center to which it is bound. Careful analysis of these nitrosyl species has led directly to the current understanding of the bonding in traditional transition metal and organometallic complexes.^{1,3} More recently, NO has been found to play crucial roles in many other chemical systems that have significant biological and environmental implications. In biological systems, NO is well-known to bind to metalloproteins as a protective step in defense against system toxins.^{4,5} In addition, NO has been implicated as an important messenger molecule in common brain functions. The environmental aspects of NO chemistry are in no way less crucial to biological systems. Since NO is a byproduct of the combustion of fossil fuels, a complete understanding of its gas phase and atmospheric chemistry is of capital importance in our modern, industrially driven society; therefore, the reactions of NO with transition metals (as found in some smogs) may provide new information by which pollution of this type can be catalytically removed.⁶ To gain a better understanding of the reactions of gas-phase transition metals with NO, we have undertaken experiments designed to investigate the products of reactions of NO with laser-ablated transition metals. The current study focuses on the products of the scandium and titanium reactions with NO. Previous studies from this laboratory have explored the analogous vanadium and chromium reactions.^{7,8}

Experimental Section

The vacuum system and cryogenic cell geometry for Nd:YAG laser ablation has been described in detail previously.^{9,10} The CsI spectroscopic window was maintained at 11–12 K by a CTI Cryogenics Model 22 cryocooler for the majority of the

Sc + NO experiments, while an APD Cryogenics closed-cycle refrigerator was used to hold the window at 7–8 K for the Ti + NO experiments. All absolute temperatures were measured by a Au/Co versus chromel thermocouple. Vapor phase scandium and titanium atoms were produced by focusing the 1064 nm fundamental of a Q-switched Spectra Physics Quanta Ray DCR-11 Nd:YAG laser onto scandium and titanium metal targets. The laser pulse duration was set at 10 ns, and the laser power at the target was varied between 5 and 40 mJ/pulse with a 10 Hz repetition rate. The scandium (Johnson-Matthey, lump, 99.9%) and titanium (Goodfellow Metals, lump, 99.99%) metal targets were mounted on a rotating (1 rpm) metal rod to avoid laser pitting of the target surface. The nitric oxide samples were prepared manometrically in molar ratios ranging from Ar/NO 100:1 to 1000:1 in order to evaluate the effect of nitric oxide concentration on the formation of products. Isotopically mixed samples (2000:1:1 and 400:1:1 $^{14}\text{NO}/^{15}\text{NO}$, $^{15}\text{NO}/^{15}\text{N}^{18}\text{O}$ and 4000:1:1:1:1 $\text{NO}/\text{N}^{18}\text{O}/^{15}\text{NO}/^{15}\text{N}^{18}\text{O}$) were also examined. The average codeposition process lasted 1–2 h with the gas spray on rate varying between 3 and 5 mmol/h. Infrared spectra were recorded on either a Nicolet 750 or a Nicolet 550 spectrometer operating with a spectral resolution of 0.5 cm^{-1} and a frequency accuracy of 0.1 cm^{-1} . Spectra were collected at the end of each deposition and before and after annealings or photolyses. Typically, each matrix was annealed quickly to 25, 35, and 40 K. Broad-band mercury arc photolysis using a medium-pressure mercury arc lamp (Philips H39KB, 175 W) with the globe removed (240–580 nm) was performed to evaluate the photosensitivity of different product species and to aid in spectral interpretation.

Computational Methods

Density functional theory calculations on suspected product species were carried out using the Gaussian94 suite of programs.¹¹ The BP86 functional¹² was used throughout, and the general methods employed for both scandium and titanium

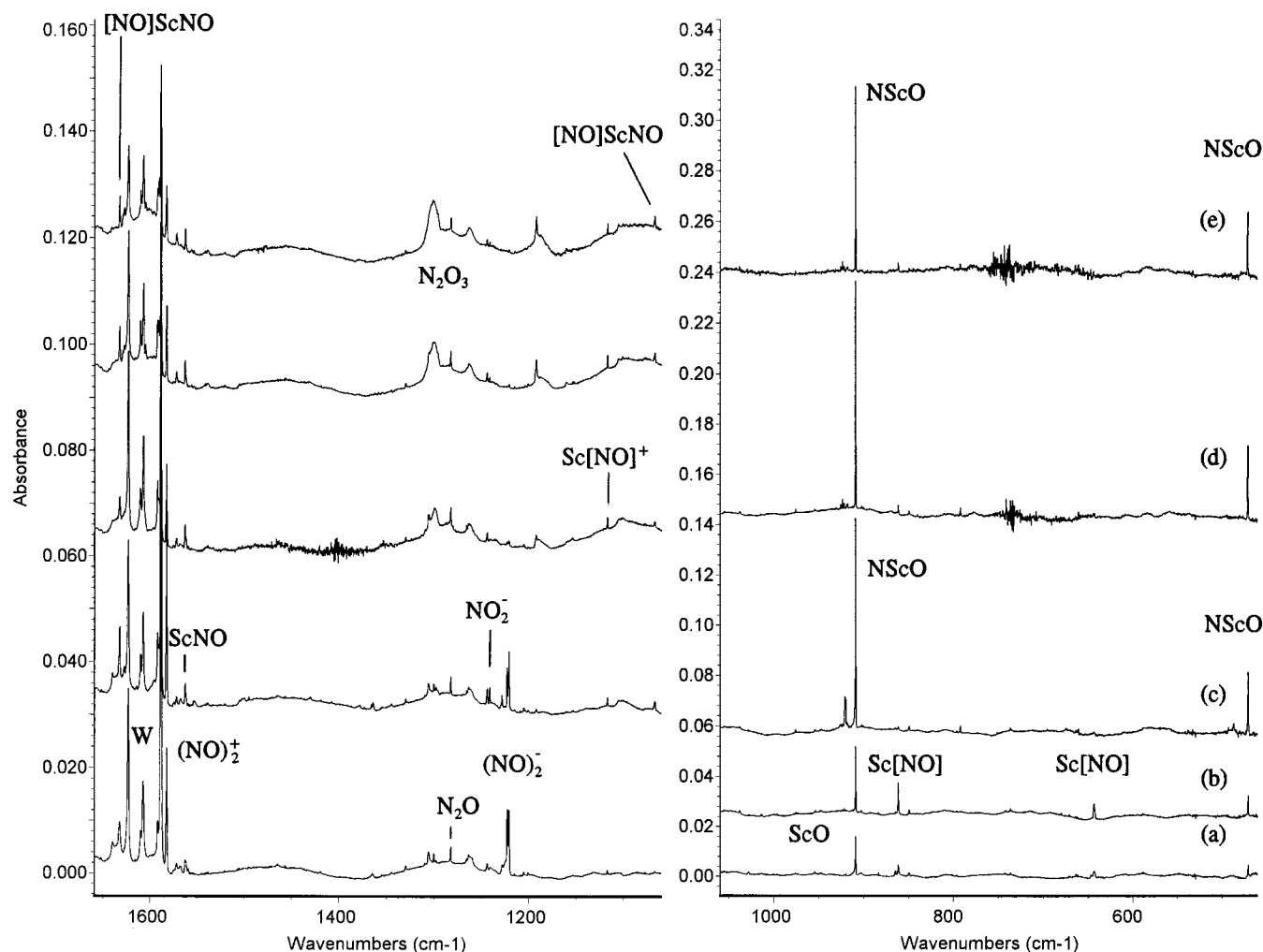


Figure 1. Infrared spectra of laser-ablated Sc atoms co-deposited with NO (0.4%) in argon at 11–12 K: (a) for 1 h; (b) after annealing to 25 K; (c) after broad-band photolysis; (d) after annealing to 30 K; (e) after annealing to 35 K.

systems were consistent with those employed for the previous investigations of the scandium oxides and nitrides.^{13,14} Briefly, the 6-31+G* basis set was used for nitrogen and oxygen,¹⁵ and the titanium and scandium sets were the (14s9p5d) set of Watchers contracted to (8s4p3d).¹⁶ In addition, the s and p spaces are contracted using contraction number 3, while the d space is contracted (311). To the Sc basis set is added one diffuse p function with exponent 0.13462; this is the tight function optimized by Wachters multiplied by 1.5. The second, more diffuse, p function is not included, as it was found to affect results very slightly, but introduced severe convergence problems to the orbital optimization procedure. The Hay diffuse d function with exponent 0.0588 is also added.¹⁷ A similar procedure is followed for Ti, thus a p function and a d function are added, with exponents of 0.15234 and 0.0720, respectively.

Results

Reaction of laser-ablated scandium and titanium atoms with nitric oxide were examined with a range of laser energies, nitric oxide concentrations, and isotopic modifications. Infrared spectra in the metal nitrosyl N–O and metal-nitride/oxide stretching regions for the products of laser-ablated scandium atoms reacting with NO in excess argon are presented in Figure 1 with isotopic modifications in Figures 2 and 3, while the associated spectra for the titanium/nitric oxide reactions are shown in Figures 4 and 5. The product absorptions are listed in Tables 1 and 2, which include bands for scandium and titanium oxide and nitride

species.^{13,14,18,19} Omitted from the tables are absorptions due to NO, (NO)₂, NO₂, N₂O, (NO)₂⁺, (NO)₂⁻, and NO₂⁻ that are common to laser-ablation experiments with NO and transition metals.^{7,8,20}

In addition, an experiment was done for each metal and NO (0.4%) in argon doped with CCl₄ (0.05%) to serve as an electron trap.²¹ These experiments gave the same primary NO reaction product absorptions and photolysis behavior plus weak CCl₄ product bands^{22,23} and enhanced (NO)₂⁺ absorptions relative to (NO)₂⁻ bands.²⁰ In addition, the 1117.0 and 976.3 cm⁻¹ bands in Sc experiments were favored with CCl₄ added, but no Ti product absorption was enhanced. Unfortunately, the 784.3 cm⁻¹ Ti-product band was masked by CCl₄.

Density functional theory (DFT) calculations have been completed for anticipated products of the scandium and titanium atom containing reactions with NO. The calculated relative energies, geometric parameters, and harmonic vibrational frequencies (not scaled) are given in Tables 3 and 4 for ScNO and TiNO species. Three isomers are possible: the side-bonded Sc[NO], the end-bonded nitrosyl ScNO, and the inserted molecule NScO. Our DFT calculations find two ring states ¹A' and ³A'' that have the same energy (within 0.06 kcal/mol); the bent inserted molecule NScO is 8.5 kcal/mol higher and the linear ScNO nitrosyl is 9.8 kcal/mol higher than the global minimum. In contrast for Ti + NO, the inserted NTiO molecule is by far the most stable isomer; the ²A' ring Ti[NO] is 20.8 kcal/mol higher, the ⁴A'' ring is +24.7 kcal/mol, and the ²Σ nitrosyl TiNO is

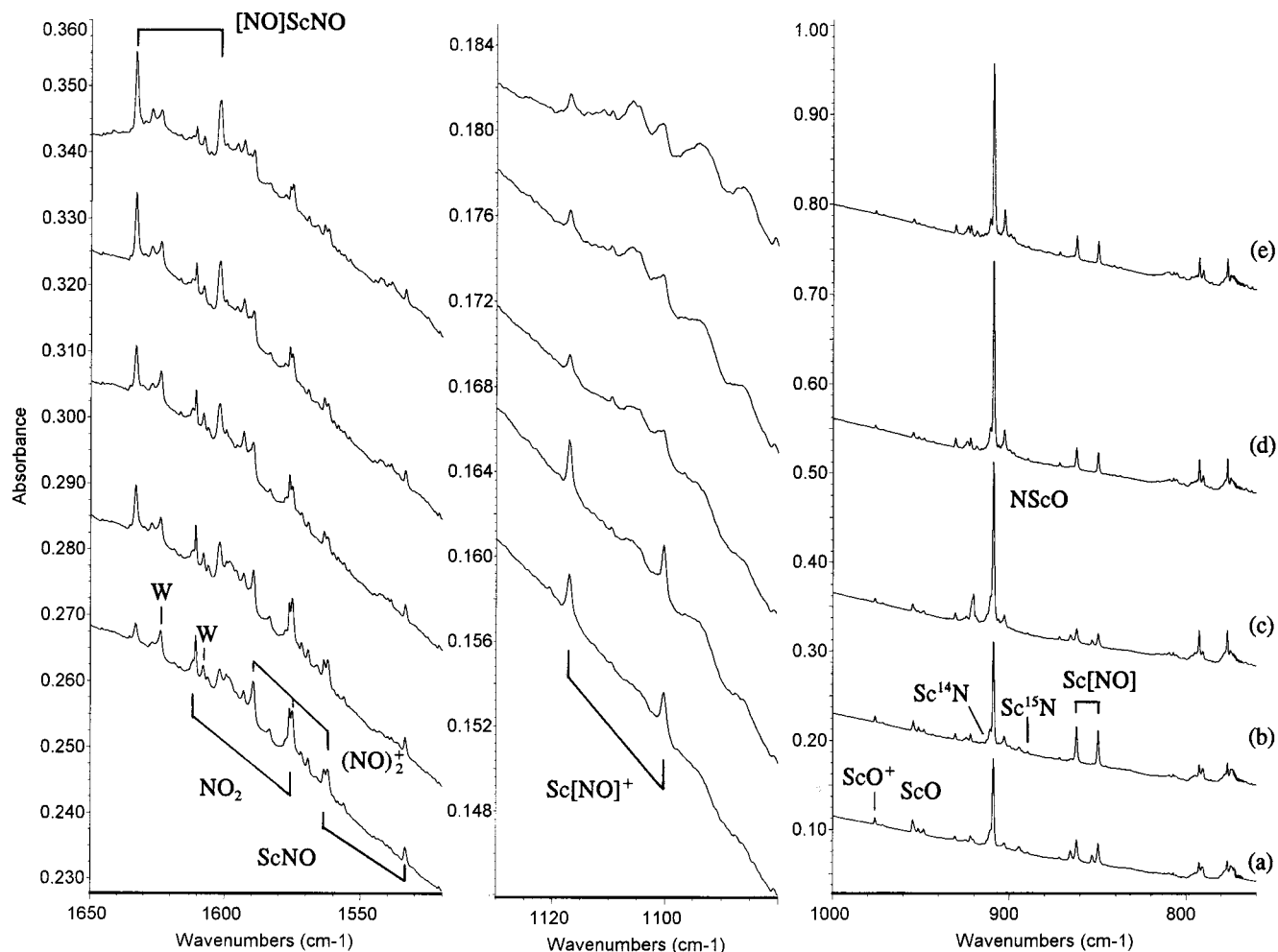


Figure 2. Infrared spectra of laser-ablated Sc atoms co-deposited with ^{14}NO (0.2%) and ^{15}NO (0.2%) in argon at 11–12 K: (a) for 1 h; (b) after annealing to 25 K; (c) after broad-band photolysis; (d) after annealing to 30 K; (e) after annealing to 35 K.

36.5 kcal/mol higher than the global minimum. The final possible forms ScON and TiON were found to optimize to the more stable cyclic isomers.

An extensive series of calculations was done for products of the $\text{Ti} + (\text{NO})_2$ reaction to help identify reaction products as well as complexes. The results are summarized in Table 5 along with calculations for $\text{Sc}(\text{NO})_2$ complexes.

Discussion

The above product absorptions will be assigned on the basis of isotopic shifts and splittings as well as by analogy with density functional theory calculations on suspected product molecules.

NScO and Sc[NO]. In a previous experimental study of the reactions of laser-ablated scandium metal with molecular oxygen,¹³ the primary reaction product, OScO , was formed by the direct insertion of the metal atom into the $\text{O}-\text{O}$ bond (although the 722.5 cm^{-1} band first identified as OScO turns out to be the electron-capture product $(\text{OScO})^-$ anion).²⁴ In contrast to the dioxygen study, the reactions of scandium with dinitrogen yield as the primary nitride product $(\text{ScN})_2$, which was produced by way of a two-step mechanism involving association of a second Sc atom to the side bound $\text{Sc}[\text{N}_2]$. There was no evidence of the direct insertion of a single Sc atom into the dinitrogen molecule triple bond.¹⁴ From this set of previous results, it is difficult to predict the primary product (products) of the NO system; however, DFT calculations provide a useful

handle and reasonable species can be predicted and henceforth identified spectroscopically. Close scrutiny of the Sc–N and Sc–O stretching regions of the infrared spectra of the matrixes formed by the co-deposition of laser ablated Sc atoms and NO diluted in argon provide evidence for two sets of bands that are produced by species having one oxygen and one nitrogen atom in their structure. The first set of absorptions is marked by an intense band at 909.5 cm^{-1} , which is observed on initial deposition and can be correlated with a weaker band at 471.1 cm^{-1} on the basis of annealing and photolytic behavior. In reactions with a mixture of $^{14}\text{N}^{16}\text{O}/^{15}\text{N}^{16}\text{O}$, the higher frequency band broadens and red shifts slightly to 909.3 cm^{-1} , while the lower frequency mode splits into a doublet ($471.1\text{--}459.3\text{ cm}^{-1}$) (Figure 2), indicating that the latter arises from the vibration of a single nitrogen atom. Co-deposition of Sc atoms with a mixture of $^{15}\text{N}^{16}\text{O}/^{15}\text{N}^{18}\text{O}$ produces infrared spectra where the higher frequency mode appears as a doublet at $909.1\text{--}871.5\text{ cm}^{-1}$, indicating the vibration of a single Sc–O bond, while the lower frequency mode exhibits very little oxygen dependence by red shifting only slightly to 459.2 cm^{-1} (Figure 3). Observation of these bands on deposition with very low laser power is consistent with a single Sc atom. These observations substantiate the stoichiometry ScNO ; however, whether these spectral features are due to the direct insertion product, NScO , or the triangle $\text{Sc}[\text{NO}]$, i.e., the side-bonded $\text{Sc}-\eta^2\text{-NO}$ complex, can only be elucidated by quantum chemical calculations, as will be outlined below.

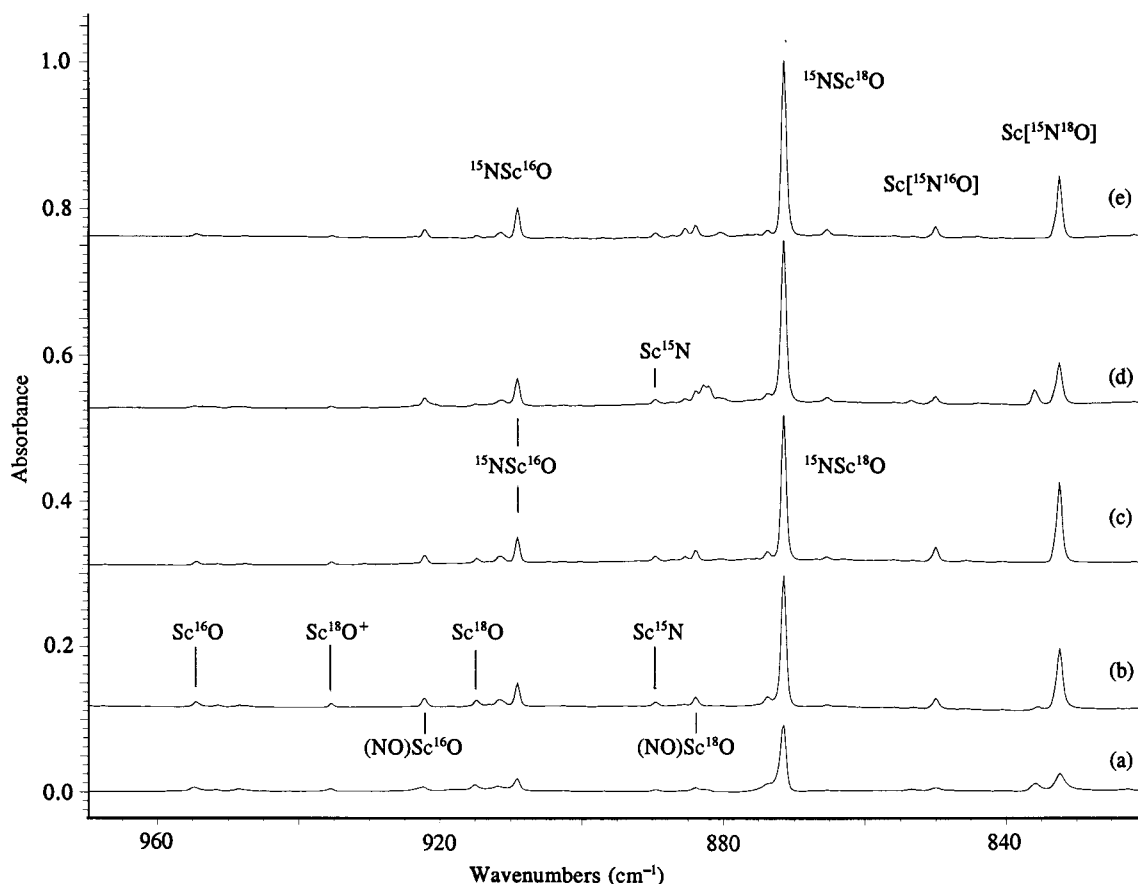


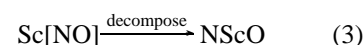
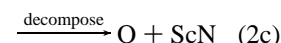
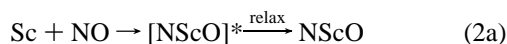
Figure 3. Infrared spectra of laser-ablated Sc atoms co-deposited with $^{15}\text{N}^{16}\text{O}$ (0.05%) and $^{15}\text{N}^{18}\text{O}$ (0.3%) in argon at 7–8 K: (a) for 1 h; (b) after annealing to 25 K; (c) after broad-band photolysis; (d) after annealing to 30 K; (e) after annealing to 35 K.

The second set of bands in this region to exhibit the vibrations of a molecule with the ScNO stoichiometry occurs at 865.5 cm^{-1} (with a site splitting at 862.0 cm^{-1}) and 644.1 cm^{-1} . In the $^{14}\text{NO}/^{15}\text{NO}$ experiments, the higher frequency absorption appears as a doublet with counterparts at 865.5 and 853.4 cm^{-1} (14/15 ratio = 1.014 18) while the lower mode also shows a significant nitrogen shift appearing as a doublet located at 644.1 and 632.9 cm^{-1} (14/15 ratio = 1.017 70). In the mixed oxygen isotope experiment, $^{15}\text{N}^{16}\text{O}/^{15}\text{N}^{18}\text{O}$, both the higher and lower frequency modes of this set appear as doublets: 853.4 – 835.9 and 633.1 – 618.8 cm^{-1} . From this information it is apparent that the two vibrational modes of this species are coupled to a much greater extent than those giving rise to the first set of bands mentioned above. Vibrational mechanics of such a mixed nature are readily attributable to a cyclic structure such as Sc[NO], while the much more isolated Sc–N and Sc–O normal coordinates exhibited by the first set of bands are characteristic of the open insertion product NScO.

BP86 calculations predict the most intense infrared absorptions for the $^3\text{A}''$ inserted NScO molecule to occur at 913.8 and 459.0 cm^{-1} , with 4 to 1 relative intensity, which are in very good agreement with the bands observed at 909.5 and 471.1 cm^{-1} with 3 to 1 relative intensity. In addition, the DFT predicted isotope ratios for the upper (16/18 = 1.043 99) and lower (14/15 = 1.026 05) modes provide sound evidence that the first set of bands is due to the NScO insertion product, as these ratios are near ratios for pure Sc–O and Sc–N vibrations, respectively. The calculations on the $^1\text{A}'$ cyclic species, Sc[NO], produce stretching frequencies at 885.3 and 641.3 cm^{-1} , once again in good agreement with the observed values at 865.5 and 644.1 cm^{-1} . As with the insertion product, the calculated potential surface for the $^1\text{A}'$ state of the Sc[NO] molecule

reproduces the observed vibrational mechanics exceptionally well. The calculated normal modes at 885.3 cm^{-1} (14/15 = 1.013 77 and 16/18 = 1.021 16) and 641.3 cm^{-1} (14/15 = 1.017 45 and 16/18 = 1.023 55) mimic almost exactly the highly mixed vibrational mode characteristics of this molecule. Note that although the $^1\text{A}'$ and $^3\text{A}''$ states of Sc[NO] have the same energy, the calculated frequencies for the $^3\text{A}''$ state are vastly different from the observed spectrum. Finally, the optimized BP86 structure for the $^1\text{A}'$ state of Sc[NO] has a shorter Sc–N bond than Sc–O bond.

Annealing and photolysis behavior of these two band sets indicate that there is a significant relationship between them. On annealing the matrix to 25 K, the features due to Sc[NO] grow 3-fold, reaction 1, and the bands due to NScO increase



$50 \pm 10\%$, reaction 2a, indicating that the formation of these species requires little or no activation energy. Since NScO is favored on deposition, its formation and decomposition are facilitated by the excess kinetic and electronic energies imparted by the laser-ablation process.²⁵

Photolysis of the matrix with a broad-band mercury arc causes the bands due to the insertion product to grow at the expense of the η^2 -bound complex, reaction 3. Such spectroscopic

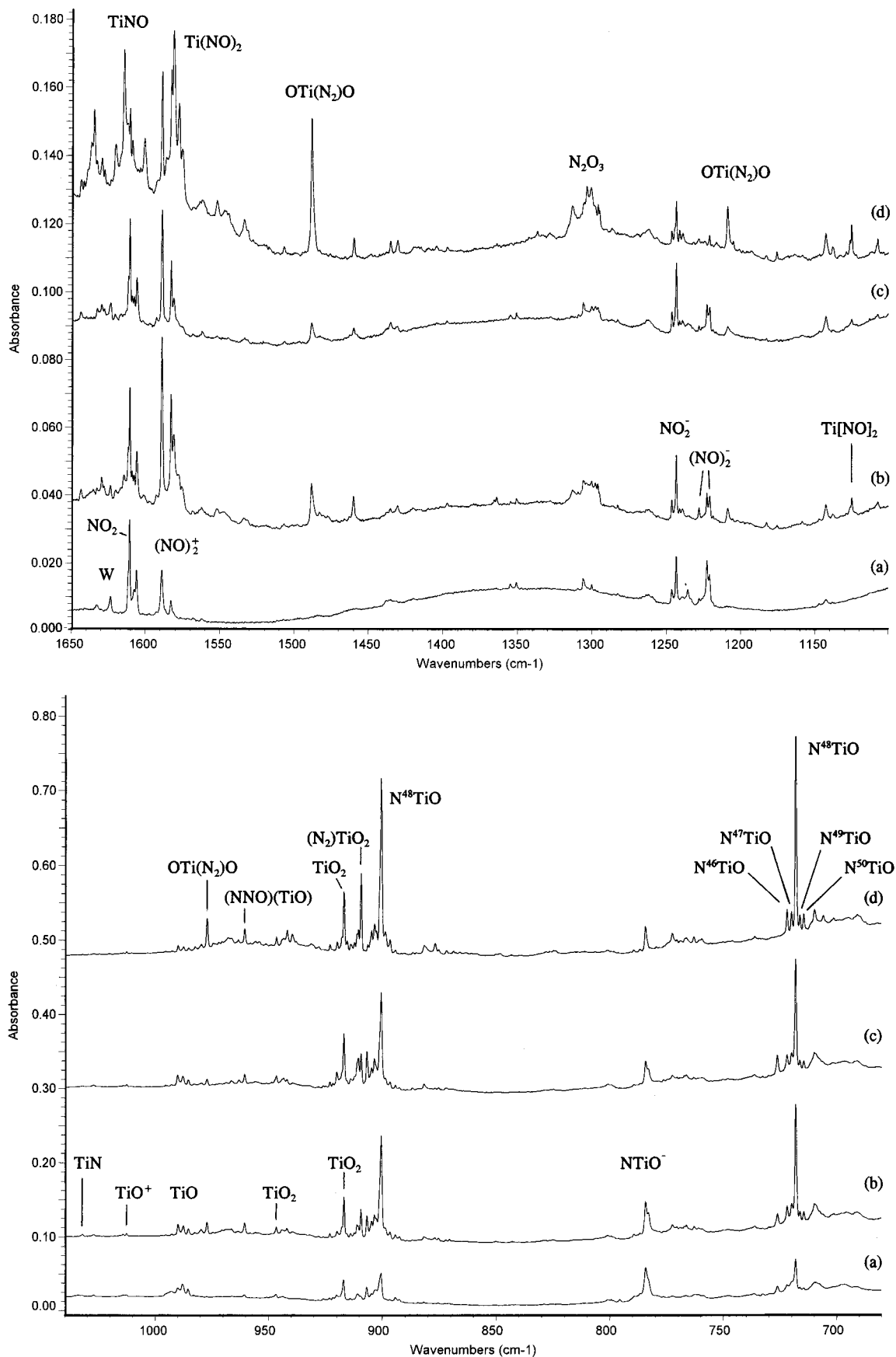


Figure 4. Infrared spectra of laser-ablated Ti atoms co-deposited with NO (0.2%) in argon at 7–8 K: (a) for 1 h; (b) after annealing to 25 K; (c) after broad-band photolysis; (d) after annealing to 36 K.

evidence indicates that Sc[NO] is photolabile toward complete N–O bond cleavage and formation of the stable open insertion product.

Note the presence of Sc¹⁶O and Sc¹⁸O at 954.8 and 915.1 cm⁻¹, which arise from the decomposition of [NScO]* before it can be relaxed by the condensing matrix, reactions 2b and

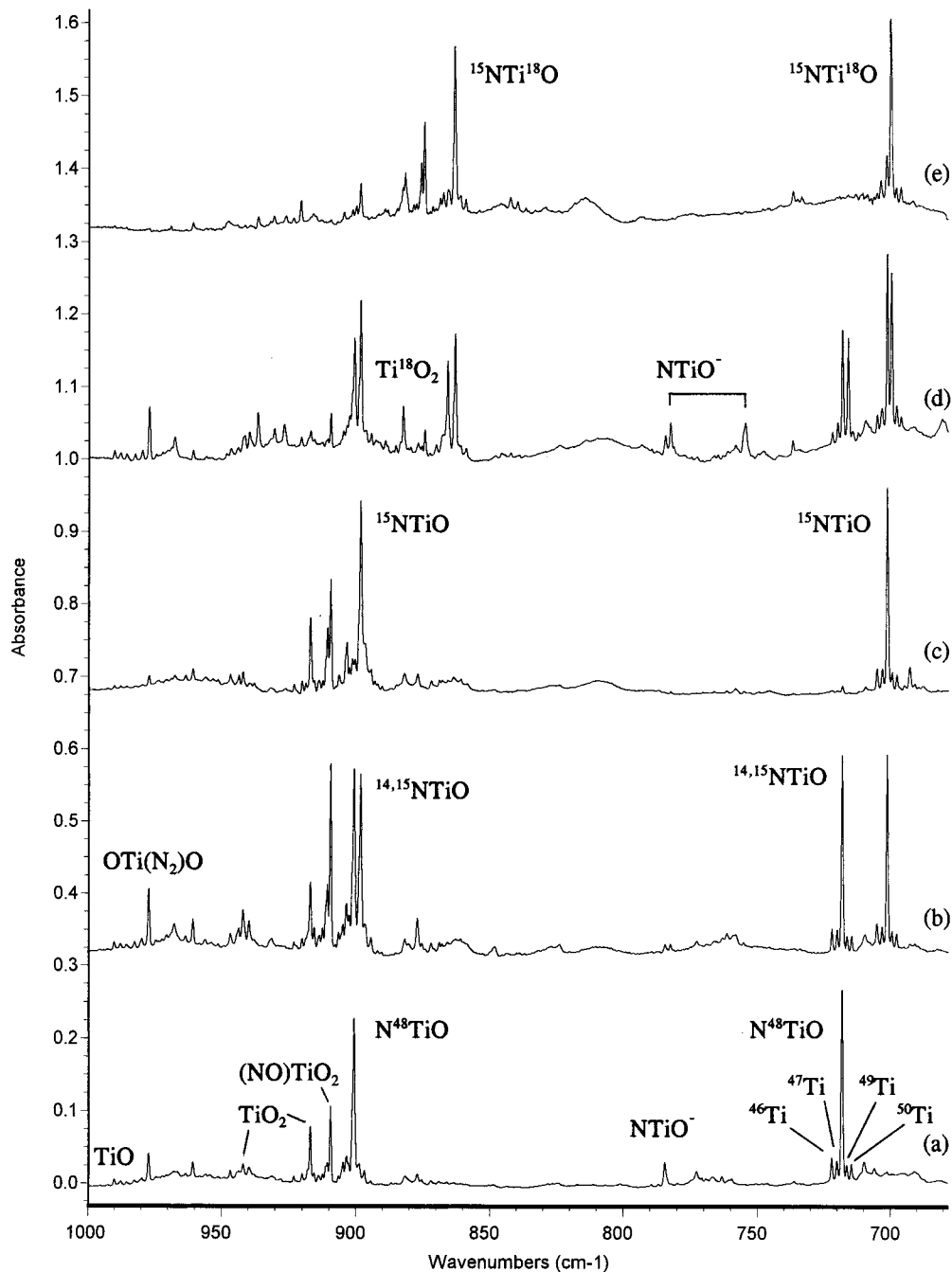


Figure 5. Infrared spectra of laser-ablated Ti atoms co-deposited with isotopic NO samples in argon at 7–8 K recorded after annealing to 34 ± 2 K: (a) 0.2% $^{14}\text{N}^{16}\text{O}$; (b) 0.15% $^{14}\text{N}^{16}\text{O}$ and 0.15% $^{15}\text{N}^{16}\text{O}$; (c) 0.2% $^{15}\text{N}^{16}\text{O}$; (d) 0.06% $^{15}\text{N}^{16}\text{O}$ and $^{15}\text{N}^{18}\text{O}$ and 0.04% $^{14}\text{N}^{16}\text{O}$ and $^{14}\text{N}^{18}\text{O}$; (e) 0.2% $^{15}\text{N}^{18}\text{O}$.

2c. Significantly, the absorptions of Sc^{14}N and Sc^{15}N at 913.0 and 889.7 cm^{-1} are exactly the same frequencies found for the Sc reaction with nitrogen.¹⁴ This observation of ScN confirms the matrix identification of the isolated ScN molecule, as N_2 was not present in these experiments and $(\text{NN})_x\text{ScN}$ complexes cannot be formed here. Note from the Sc^{15}N and Sc^{18}O product band yields in Figure 3 that the ScN decomposition product is favored over the ScO product (oscillator strengths make this preference an order of magnitude more for ScN).^{13,14} The energized $[\text{NScO}]^*$ intermediate may have a stronger ScN bond, in contrast to the relaxed NScO product.

NTiO. As with the above scandium example, laser-ablated titanium also reacts with NO to give the metal insertion product NTiO, which follows the reaction with dioxygen in contrast to the reaction with dinitrogen.^{18,19} The formation of this species

in the Ar/NO matrix experiments is confirmed by the two sharp bands at 900.6 and 718.2 cm^{-1} . These absorptions can be grouped to a single molecule by noting their consistent behavior upon photolysis and annealing (Figure 4) and sample dilution over an order of magnitude. Annealing the matrix to 25 K causes a growth in intensity of these features by a factor of 5, while photolysis decreases their intensity by approximately 10%. The slight growth of TiN, TiO, and TiO_2 on 25 K annealing prompted lower temperature annealing in separate low laser power experiments. It was found that annealing to 14 K produced a 20% increase in both NTiO bands and a 5% increase in $(\text{NO})_2$ without an increase in N_2O , O_3 , TiO, or TiO_2 absorptions. Hence, we assume that 14 K represents the onset of diffusion of Ti and/or NO in solid argon and that at 14 K the

TABLE 1: Observed Vibrational Frequencies (cm⁻¹) for Matrix-isolated Species Produced by Reactions of Laser-Ablated Scandium Atoms with Nitric Oxide Diluted in Argon

product species	NO	NO/ ¹⁵ N ¹⁶ O	¹⁵ NO	¹⁵ NO/ ¹⁵ N ¹⁸ O	¹⁵ N ¹⁸ O
[NO]ScNO	1633.2	1633.2, 1601.8	1601.8	1601.8, 1563.7	1563.7
ScNO	1563.3	1563.3, 1533.6	1533.6	1533.6, 1497.1	1497.1
Sc ₂ NO?	1192.3	1192.3, 1149.6	1149.6	1149.6, 1140.3	1140.3
Sc[NO] ⁺	1117.0	1117.0, 1100.2	1100.2	1100.2, 1069.8	1069.8
[NO]ScNO	1067.1	1066.9, 1056.8	1056.7	1056.7, 1022.1	1022.1
ScO ⁺	976.3	976.3	976.3	976.3, 935.6	935.6
ScO	954.8	954.8	954.8	954.8, 915.1	915.1
(NO)ScO	920.6	920.6	920.6	920.6, 882.1	882.1
ScN	913.0	913.0, 889.7	889.7	889.7	889.7
NScO	909.5	909.3	909.1	909.1, 871.5	871.5
NScO (NO)	903.2	903.1	903.0	903.0, 865.5	865.5
Sc[NO]	865.5	865.5, 853.4	853.4	853.4, 835.9	835.9
Sc[NO] (site)	862.0	862.0, 850.0	850.0	850.0, 832.4	832.4
Sc _x N _y O _z ?	792.5	792.5, 776.4	776.4	776.4, 769.8	769.8
Sc _x N _y O _z ?	790.3	790.3, 774.7	774.7	774.7, 774.7	768.3
Sc[NO]	644.1	644.1, 632.9	632.9	633.1, 618.8	618.8
NScO	471.1	471.1, 459.3	459.3	459.2	459.1

Ti + NO reaction is spontaneous. Further annealings to 16 and 18 K produced an additional 50% increase in both NTiO absorptions.

In the reactions of Ti with a ¹⁴N¹⁶O/¹⁵N¹⁶O mixture, the higher frequency band splits into a very closely spaced doublet (900.6–898.2 cm⁻¹), as does the lower frequency mode, but with a much greater separation (718.2–701.2 cm⁻¹) (Figure 5). In the reactions of Ti with a ¹⁵N¹⁶O/¹⁵N¹⁸O mixture, very similar results are recorded with both bands appearing as doublets: 898.2–862.9 cm⁻¹ and 701.2–699.7 cm⁻¹. Figure 5d shows the spectrum with four isotopic precursors: four band pairs were observed, the three pairs just mentioned and 865.7, 716.0 cm⁻¹ for the ¹⁴N¹⁸O reaction. It is evident from the magnitudes of the isotopic splittings given above that the higher frequency vibration of this species is primarily a Ti–O stretching coordinate while the lower mode is primarily Ti–N in character. The fact that each of the vibrational modes occurs as a doublet in each of the mixed isotope experiments indicates that this species contains a single nitrogen and a single oxygen atom.

In addition to the oxygen and nitrogen isotopic substitutions, the primarily Ti–N vibration of this molecule gives rise to an absorption of sufficient intensity and sharpness to allow for resolution of titanium isotopic splittings. Sharp satellite features at 721.9, 720.0, 716.3, and 714.5 cm⁻¹ about the very intense 718.2 cm⁻¹ band in the Ti + NO spectra (Figures 4 and 5) are due to Ti–N vibrations of the N⁴⁶TiO, N⁴⁷TiO, N⁴⁹TiO, and N⁵⁰TiO species with the most intense absorption due to the N⁴⁸TiO isotopic counterpart. The natural titanium isotopic splittings on this mode and the 1.33:1.33:12.33:1.00:1.00 pentet formed by these features prove that only one titanium atom is present in this species. All of the above data confirm that the molecule giving rise to these features has the stoichiometry NTiO.

As with NScO, BP86 calculations on the NTiO molecule predict a bent structure. Frequency calculations on the ground ²A' state produce vibrational modes at 936.3 and 761.1 cm⁻¹, which are in reasonable agreement with the observed frequencies. Of more importance, the isotope shifts are reproduced to substantial accuracy (within 1.7, 0.5, 0.3, and 2.6 cm⁻¹) by the DFT vibrational potential, and the two band intensities are the same (within 10%) as predicted, illustrating a very good match between observed and calculated normal mode descriptions (the calculations slightly overestimate the mode mixing). Finally, the DFT frequency calculations confirm assignment of the above

spectral features to the Ti–O and Ti–N stretching vibrations of the bent NTiO molecule, respectively.

One means of understanding this interesting NTiO molecule is to compare its interaction with solid argon and neon hosts, and to this end, several neon experiments were performed. The NTiO bands were observed at 914.9 and 731.9 cm⁻¹ along with a weak 936.5 cm⁻¹ TiO₂ band. The argon-to-neon blue shifts for NTiO (14.3, 13.7 cm⁻¹) are smaller than the blue shift (20 cm⁻¹) for TiO₂.

It is interesting to note that there is no evidence for the formation of a Ti[NO] complex analogous to that observed in the scandium experiments. Our BP86 calculations predict this species to have a ²A' ground state, much like NTiO, but to lie 20.8 kcal mol higher in energy than the insertion product. These results indicate that unlike the scandium species, the η²-bound titanium product is most likely unstable with respect to direct Ti insertion into the N–O bond. This postulate is supported by the onset of growth on annealing to 14 K and the remarkable 5-fold increase observed in the NTiO bands upon annealing to 25 K in solid argon. This growth is indicative of the absence of any activation barrier to direct Ti insertion into the N–O bond, reaction 4a.



It can be argued that the insertion reaction in the Ti system is certainly driven to some extent by the strength of the Ti–N bond formed relative to the Sc–N bond in the Sc insertion product. In the Sc + NO system, the low Sc–N bond stretching frequency in NScO (471.1 cm⁻¹) indicates a very weak Sc–N bond, while in the Ti system, the Ti–N stretching coordinate occurs at a significantly higher energy (718.2 cm⁻¹). The relative strength of the Ti–N bond in NTiO arises as a result of the extra electron in the titanium system lying almost exclusively in the bonding orbitals between the Ti and N atoms stabilizing the open-chain insertion product. In contrast, the electron deficient Sc–N bond in the Sc + NO system benefits from the delocalized orbitals in the cyclic, η²-bound, Sc[NO] molecular form, thereby stabilizing this species with respect to NScO.

Some of the energized (NTiO)* first formed decomposes, as TiO and TiN (Ti¹⁵N and Ti¹⁸O) are observed as minor reaction products, reactions 4b and 4c.^{18,19} This is significant for the assignment of isolated TiN at 1034.1, 1032.4 cm⁻¹ from N atom reactions in the presence of N₂, which can form (NN)_xTiN complexes.¹⁹

The greater strength of the metal–oxygen bonds as compared to the metal–nitrogen bonds in NScO and NTiO is shown not only by the calculated bond lengths and frequencies (Tables 3 and 4) but also by comparison with the diatomic frequencies of ScO (954.8 cm⁻¹), ScN (913.0 cm⁻¹) and TiO (988.0 cm⁻¹), TiN (1032.4 cm⁻¹).^{13,14,18,19} It is seen that the M–O stretching modes in NScO and NTiO are only 67 ± 21 cm⁻¹ below the diatomic oxides whereas the M–N vibrations are 378 ± 64 cm⁻¹ lower than the diatomic nitrides.

This contrasts the bent NVO and NCrO molecules, which have more d electrons and can satisfy the nitride requirement. In these cases the metal–nitride stretching frequencies are higher than the metal–oxide modes, and DFT calculations show that the M–N bonds are shorter than the M–O bonds.^{7,8}

Metal Nitrosyl Complexes. Although the mixed nitride–oxide species discussed above appear to be the preferred products of the reactions of the excited metal atoms produced

TABLE 2: Observed Vibrational Frequencies (cm⁻¹) for Matrix-isolated Species Produced by Reactions of Laser-ablated Titanium Atoms with Nitric Oxide Diluted in Argon

product species	NO	NO/ ¹⁵ NO	¹⁵ NO	¹⁵ NO/ ¹⁵ N ¹⁸ O	¹⁵ N ¹⁸ O
(NNO)(TiO)	2301.9		2229.4 site		2222.8
(NNO)(TiO)	2294.2	2294.2, 2271.8, 2246.2, 2223.3	2223.3		2215.3
Ti _x (NO) _y	1635.1		1606.7		1563.7
TiNO	1614.7		1586.0		1544.3
Ti _x (NO) _y	1600.9		1572.9		1531.5
Ti(NO) ₂	1581.3	1581.3, 1565.4, 1552.9	1552.9		1510.7
OTi(N ₂)O	1488.5	1488.5, 1479.2, 1456.5	1448.7	1448.7, 1435.1	1435.1
OTi(N ₂)O	1208.8	1208.8, 1195.7, 1191.8, 1178.8	1178.8	1178.8, 1160.9	1160.9
Ti _x [NO] _y	1142.6		1122.4		1095.9
Ti[NO] ₂	1125.1	1125.1, 1113.9, 1104.6	1104.6	1104.6, 1092, 1075.8	1075.0
TiN	1034.1	1034.0, 1007.5	1007.4		
TiN	1032.4	1032.5, 1005.8	1005.7		1005.8
TiO ⁺	1014.3	1014.3	1014.3	1014.3, 971.2	971.2
TiO ⁺	1012.7	1012.7	1012.7	1012.7, 969.8	969.8
TiO	988.0	988.0	988.0	988.0, 947.5	947.5
OTi(N ₂)O	977.1	977.1	977.1	977.1, 936.4	936.4
(NNO)(TiO)	963.3		963.3		923.2
(NNO)(TiO)	960.6		960.6	960.5, 920.4	920.4
OTiO (ν ₁)	946.8	948.6	946.8		904.5
(N ₂)(TiO ₂) (ν ₁)	941.9	941.9	941.9		898.2
OTiO (ν ₃)	916.8		916.9	916.9	881.7
(N ₂)(TiO ₂) (ν ₃)	909.3	909.3	909.3	909.3, 882.3, 874.3	874.3
NTiO	900.6	900.6, 898.2	898.2	898.1, 862.9	862.9
(NTiO) ⁻	784.3	784.3, 782.4	782.4	784.3, 782.4,	754.5
			754.6 (br)		
NTiO	718.2	718.2, 701.2	701.2	701.2, 699.7	699.7

TABLE 3: Relative Energies (kcal/mol), Geometries, Isotopic Frequencies (cm⁻¹), Intensities (km/mol) and Isotopic Frequency Ratios Calculated for ScNO Species Using the BP86 Density Functional

molecule	energy	geometry	14–16 (<i>I</i>)	15–16	15–18	R(14–16/15–16)	R(15–16/15–18)
Sc[NO]	0.00	Sc–N = 1.814 Å	885.3 (65)	873.3	855.2	1.013 74	1.021 16
¹ A'		Sc–O = 1.840 Å	641.3 (31)	630.3	615.8	1.017 45	1.023 55
		N–O = 1.524 Å	490.1 (4)	483.7	471.2	1.013 23	1.026 53
Sc[NO]	+0.06	Sc–N = 1.951 Å	1091.3 (134)	1073.2	1042.8	1.016 87	1.029 15
³ A''		Sc–O = 1.950 Å	601.8 (14)	589.7	586.7	1.020 52	1.005 11
		N–O = 1.345 Å	480.8 (5)	477.2	459.5	1.007 54	1.038 52
NScO	+8.5	Sc–N = 2.112 Å	913.83 (171)	913.73	875.22	1.000 11	1.043 99
³ A''		Sc–O = 1.699 Å	458.95 (44)	447.30	447.26	1.026 05	1.000 09
		∠NScO = 112.7°	152.4 (26)	150.6	146.8	1.011 95	1.025 89
ScNO	+9.8	Sc–N = 1.856 Å	1543.8 (442)	1513.4	1477.0	1.020 09	1.024 64
³ Π		N–O = 1.230 Å	568.0 (3)	563.5	551.4	1.007 99	1.021 94
		linear	280.9 (44)	274.0	270.3	1.025 18	1.013 69
NScO	+24.5	Sc–N = 1.721 Å	884.9 (176)				
¹ Σ		Sc–O = 1.740 Å	698.5 (7)				
		linear	90.8 (2 × 112)				
Sc[NO] ⁺	+150.6	Sc–N = 1.912 Å	1146.9 (90)	1128.2	1096.2	1.016 58	1.029 19
² A''		Sc–O = 1.923 Å	612.5 (11)	599.3	596.6	1.022 03	1.004 53
		N–O = 1.325 Å	493.1 (7)	490.0	471.6	1.006 33	1.039 02
ScNO ⁺	+151.2	Sc–N = 1.845 Å	1641.1 (269)	1609.5	1569.4	1.019 63	1.025 55
² Π		N–O = 1.204 Å	583.4 (9)	578.5	566.6	1.008 47	1.036 89
		linear	308.7 (77)	301.1	297.0	1.025 24	1.013 47
NScO ⁺	+222.0	Sc–N = 2.210 Å	837.0 (28)	836.7	800.5	1.000 36	1.045 22
² A''		Sc–O = 1.685 Å	321.1 (13)	312.8	312.7	1.026 53	1.000 32
		∠NScO = 135.8°	86.3 (38)	79.5	77.6	1.010 06	1.024 48
ScNO ⁻	-19.7	Sc–N = 1.875 Å	140.6 (420)				
doublet		N–O = 1.254 Å	541.7 (8)				
		linear	264.6 (2 × 3)				
Sc[NO] ⁻	-25.6	Sc–N = 1.943 Å	943.0 (479)	927.2	904.6	1.017 04	1.024 98
doublet		Sc–O = 1.958 Å	475.9 (10)	469.6	455.3	1.013 42	1.031 41
		N–O = 1.390 Å	188.0 (671)	185.2	182.5	1.015 12	1.014 79
NScO ⁻	-30.4	Sc–N = 1.939 Å	783.9 (71)	787.7	750.4	1.001 53	1.043 04
² A'		Sc–O = 1.775 Å	446.7 (168)	435.3	435.0	1.026 19	1.000 69
		∠NScO = 117.4°	135.2 (7)	133.8	130.6	1.010 46	1.024 50

by the laser-ablation process with NO, postdeposition aggregation as a result of matrix annealing tends to provide conditions favorable to the formation of metal nitrosyl molecular complexes. Reactions of cold Sc atoms with NO in an argon matrix give rise to new absorptions at 1633.2 and 1563.3 cm⁻¹ for possible ScNO nitrosyl complexes. These absorptions grow slightly on annealing and are relatively unaffected by photolysis.

This behavior is consistent with the growth of other molecular complexes in similar matrix experiments.^{7,8} In the reactions of Sc with a mixture of ¹⁴N/¹⁵N in argon the above absorptions appear as doublets at 1633.1–1601.8 and 1563.3–1533.6 cm⁻¹, indicating the presence of a single nitrogen atom in this species. From the large ¹⁴N/¹⁵N isotopic ratios (1.019 54 and 1.019 37) and small ¹⁶O/¹⁸O ratios (1.024 37 and 1.024 38) compared to

TABLE 4: Relative Energies (kcal/mol), Geometries, Isotopic Frequencies (cm⁻¹), Intensities (km/mol), and Isotopic Frequency Ratios Calculated for TiNO Species

molecule	energy	geometry	14–16 (<i>I</i>)	15–16	15–18
NTiO	0.0	Ti–O = 1.661 Å	936.3 (83)	932.2	897.4
² A'		Ti–N = 1.715 Å	761.1 (84)	744.4	740.3
		∠NTiO = 105.8°	246.5 (17)	243.1	237.6
Ti[NO]	+20.8	Ti–O = 1.737 Å	966.8 (120)	952.4	932.1
² A'		Ti–N = 1.781 Å	708.2 (27)	695.7	680.0
		N–O = 1.467 Å	512.6 (2)	506.6	493.3
TiNO	+36.5	Ti–N = 1.713 Å	1600.3 (678)		
² Σ		N–O = 1.228 Å	633.1 (0)		
		linear	344.8 (2 × 21)		
Ti[NO]	+39.4	Ti–O = 1.945 Å	1166.0 (199)		
⁴ A''		Ti–N = 1.893 Å	624.3 (17)		
		N–O = 1.320 Å	442.0 (9)		
NTiO	+51.4	Ti–O = 1.662 Å	911.3 (124)		
⁴ A''		Ti–N = 1.930 Å	541.0 (37)		
		∠NTiO = 141.5°	130.1 (40)		
Ti[NO] ⁺	+186.2	Ti–O = 1.756 Å	1038.4 (46)		
¹ A'		Ti–N = 1.700 Å	736.6 (18)		
		N–O = 1.398 Å	521.9 (2)		
TiNO ⁺	+197.4	TiN = 1.805 Å	1718.0 (330)		
³ φ		N–O = 1.191 Å	577.2 (6)		
		linear	303.6 (2 × 26)		
NTiO ⁻	-33.6	Ti–O = 1.735 Å	901.1 (48)	884.3	871.8
¹ A'		Ti–N = 1.689 Å	752.6 (935)	746.6	726.4
		∠NTiO = 111.8°	291.6 (35)	287.5	281.0

TABLE 5: Relative Energies (kcal/mol), Structures, Stretching Frequencies (cm⁻¹), and Intensities (km/mol) Calculated for Sc and Ti Plus (NO)₂ Product Species Using the BP86 Density Functional

	energy	frequencies (intensities)
Sc + (NO) ₂		
side, side, ² A'	0.0	1240.1 (62), 1148.4 (599)
side, end, ^a doublet	+0.4	1642.7 (488), 1076.7 (290)
end, end, ² A''	+5.6	1654.2 (415), 1546.2 (1087)
Ti + (NO) ₂		
side, side, ¹ A'	0.0	1197.2 (50), 1144.2 (372)
(NTiO)(NO), triplet	+2.1	1784.4 (524), 914.8 (94), 671.4 (52)
end, end, ³ B ₁	+7.0	1631.3 (121), 1549.0 (1870)
end, end, ¹ A ₁	-4.5	1675.6 (201), 1590.0 (1123)
side, end, singlet	-5.3	1632.3 (718), 1149.6 (257)
OTi(N ₂)O, triplet	-24.6	1713.3 (218), 1174.2 (185), 995.7 (207)
TiONNO, triplet	-27.2	1783.6 (302), 1240.8 (375), 1001.6 (222)
OTiNNO, singlet	-30.3	1393.2 (507), 1142.4 (12), 954.2 (249)
		1366.4, 1110.0, 994.8 ^b
		1332.8, 1101.6, 953.8 ^c
OTi(N ₂)O, singlet	-47.3	1523.6 (466), 1174.7 (59), 1005.0 (210)
		1486.0, 1143.3, 1004.9 ^b
		1463.4, 1129.2, 962.4 ^c
(NN)TiO ₂ , singlet	-112.8	2311.7 (83), 961.2 (25), 912.9 (289)

^a Side and end denote side-bonded η²-NO and end-bonded η¹-NO, respectively. ^bFrequencies for (15–16)₂ product. ^c Frequencies for (15–18)₂ product.

NO (1.017 95 for 14/15 and 1.027 72 for 16/18) it is evident that these bands are produced by a nitrogen motion that is somewhat antisymmetric in character, consistent with the N–O stretching vibration of an Sc–N–O type of species. These modes appear as doublets in the Sc + ¹⁵NO/¹⁵N¹⁸O experiment, confirming the participation of a single oxygen atom in this vibration and providing further evidence that these bands are due to the ScNO subunit.

DFT calculations at the BP86 level of theory indicate that the ScNO complex has a linear structure with a ³Π ground electronic state and that ScNO⁺ has a linear ²Π ground state, in agreement with other workers.^{26,27} Vibrational calculations on these species predict the most intense vibrational modes to occur at 1543.8 and 1641.1 cm⁻¹, respectively (Table 3). The 1563.3 cm⁻¹ band is assigned accordingly to ScNO. New

experiments in progress with Sc and O₂ show that the 976.3 cm⁻¹ band is due to ScO⁺ and provide further evidence for Sc⁺ cation as well as Sc atom reactions in these laser ablation experiments.^{13,24} Although the 1633.2 cm⁻¹ band could be due to ScNO⁺, its survival on the highest annealing and lack of enhancement with doped CCl₄ cast doubt and suggest grouping with the 1067.1 cm⁻¹ band below.

In the Ti + NO spectra, the region typically associated with the N–O stretching coordinates of titanium nitrosyl complexes reveals more bands than the analogous spectral region in the Sc + NO spectra. The high density of features in this range makes unambiguous assignment of these bands difficult; however, bands that can be assigned with confidence to titanium nitrosyl complexes occur at 1635.1, 1614.7, and 1581.3 cm⁻¹. The new product bands can be separated from previously observed absorptions on the basis of their individual photolytic and annealing behaviors in the pure isotopic experiments, but in the mixed isotope experiments, it is difficult to identify all of the components of a given bandset with ultimate confidence. Fortunately, the BP86 calculations provide additional information to aid in band assignment. Our DFT calculations predict the N–O fundamental of the ²Σ of the linear mononitrosyl complex (TiNO) at 1600.2 cm⁻¹, again in agreement with previous work,²⁷ indicating that all of the above absorptions occur in the proper frequency region to be due to a nitrosyl complex of titanium.

In the ¹⁴NO/¹⁵NO experiments, the band at 1614.7 cm⁻¹ is the only feature that is obviously a doublet (1614.7–1586.0 cm⁻¹); therefore, it is assigned to the TiNO complex. The ¹⁴N/¹⁵N isotope ratio for this feature (1.018 09) is somewhat higher than the associated ratio in the NO molecule (¹⁴NO/¹⁵NO = 1.017 95) which is consistent with an N-bound, η¹-nitrosyl complex. Further support for this assignment comes from the loss of O atom participation in this vibration (¹⁶O/¹⁸O = 1.027 00) relative to that in the free NO molecule (¹⁵N¹⁶O/¹⁵N¹⁸O = 1.027 72) and the appearance of a doublet of bands due to this species in the ¹⁵NO/¹⁵N¹⁸O experiments (1586.0–1544.3 cm⁻¹), providing proof that this is a single nitrosyl species. The density functional calculations indicate that the end-bound TiNO molecule is the highest energy structure having this stoichiometry, with the above-mentioned ²Σ electronic state lying 15.7 kcal/mol above the ²A', η²-bound complex, which is unobserved in these experiments, and 36.5 kcal/mol above the NTiO insertion product.

NTiO⁻. One of the more interesting findings of the present study is that Sc and Ti metals form stable insertion products with NO even though none of these metal centers contain enough valence electrons to support both a true nitride and a true oxide bond. The effects of the electron deficiency in these products are evidenced by the low vibrational frequency for the primarily M–N stretching modes for these species. This frequency drop indicates a significant loss of electron density in the M–N bonding orbitals *versus* that in the ScN and TiN mononitrides. In the case of titanium, the addition of a single electron to the NTiO species produces an anion that is isoelectronic with OTiO, a molecule that has been thoroughly studied and is well-known to be exceptionally stable.^{18,28} In the laser-ablation experiment, apart from atomic species, electrons are also ablated and can be captured by species such as NTiO to form stable anions in the argon matrix. This process has been well documented in previous laser-ablation experiments, and the fact that the cis and trans (NO)₂⁻ anions are formed under the present experimental conditions is further support for the production of electrons during the ablation process.²⁰

In the spectrum of the reactions of Ti with natural abundance NO, the medium intensity band at 784.3 cm^{-1} can be associated with the molecular anion $(\text{NTiO})^-$. This mode is primarily a Ti–O stretching mode, which shows slight coupling to nitrogen; this mode shifts to 782.5 cm^{-1} when the nitric oxide precursor is labeled with ^{15}N , and undergoes a further 27.9 cm^{-1} shift to 754.6 cm^{-1} in the Ti + $^{15}\text{N}^{18}\text{O}$ experiments. In the reactions of titanium with a mixture of all possible NO isotopomers, this feature splits into an asymmetric quartet of bands: 784.3 – 782.5 – 754.6 (br), in which the lowest frequency feature is an unresolved doublet (Figure 5). These features are at their maximum intensity in the spectrum collected directly following deposition and decrease slightly on annealing. Upon photolysis, this feature is decreased (Figure 4) or destroyed (^{15}NO experiments), a behavior consistent with charged species in matrix experiments.²⁰ This extreme photosensitivity, in conjunction with the obvious isotope splittings, provides reasonable evidence that this feature may be due to the NTiO^- anion. The neon matrix counterpart is blue shifted to 790.9 cm^{-1} for this possible closed-shell anion, even less than found for the open-shell neutral NTiO molecule.

Density functional calculations on the NTiO^- species predict a $^1\text{A}'$ electronic ground state, which is analogous to the electronic structure of the OTiO molecule (see Table 4). Vibrational frequency calculations at this level of theory indicate that only one mode, at 752.6 cm^{-1} , gives rise to an absorption that is of significant enough infrared intensity to be observed. This mode is in reasonable agreement with the observed band at 784.3 cm^{-1} . The vibrational mechanics of the experimentally observed feature indicate that it is a primarily TiO stretching mode, which is also borne out by the calculations; however, the mode mixing produced by the DFT vibrational force field is slightly more than is observed; i.e., the ^{15}N shift in this mode is predicted to be approximately 6 cm^{-1} , while the experimentally observed shift is only about 1.8 cm^{-1} . Although small, this type of discrepancy in isotope shift magnitude and mixing can often be caused by the inability of the single reference DFT method used here to correctly model the complicated, multi-configurational nature of the wave function of the molecule in question. Regardless, the results of the calculation provide support for the present assignment to NTiO^- .

Another isoelectronic molecule, NVO, has been observed and the lower V–O stretching mode (906.4 cm^{-1}) is stronger than the higher V–N vibration (998.1 cm^{-1}).⁷ Furthermore, the same type of DFT calculations predict an $^1\text{A}'$ ground state with a stronger, lower frequency V–O stretching mode for NVO, similar to that observed and calculated here for the NTiO^- anion.

$\text{Sc}[\text{NO}]^+$. The weak 1117.0 cm^{-1} band decreases on annealing and on photolysis and is substantially enhanced by CCl_4 doping. This band shifts to 1100.2 cm^{-1} with ^{15}NO and gives a doublet with the isotopic mixture. In addition, the band is displaced to 1069.8 with $^{15}\text{N}^{18}\text{O}$ and yields a doublet using the isotopic mixture. Clearly one NO subunit is involved in this vibrational mode. Examination of Table 3 finds a possible match for $\text{Sc}[\text{NO}]^+$ with calculated strong absorption at 1146.9 cm^{-1} , 14/15 isotopic ratio 1.016 58, and 16/18 isotopic ratio 1.029 19. The isotopic ratios observed for the 1117.0 cm^{-1} band, 1.015 27 and 1.028 42, are in very good agreement with the calculated values and support this identification of $\text{Sc}[\text{NO}]^+$, the most stable cation isomer.²⁶

The $\text{Sc}[\text{NO}]^+$ cation is probably made by direct reaction 5 during sample deposition with Sc^+ from the laser ablation process.²⁵ The role of CCl_4 in the doped experiment is to capture electrons and allow both Sc^+ and $\text{Sc}[\text{NO}]^+$ to survive the



deposition process. In addition, with CCl_4 present, the $\text{Sc}[\text{NO}]^+$ absorption increases a factor of 3 on photolysis, which decreases $\text{Sc}[\text{NO}]$ and produces NScO . The same photolysis behavior has been found in this laboratory²⁹ for $\text{OSc}[\text{CO}]$, OScCO , and OScCO^+ . This dramatic increase in $\text{Sc}[\text{NO}]^+$ on photolysis is probably due to sequential two photon ionization involving an intermediate state. In this regard, the 976.3 cm^{-1} band in Sc experiments is also enhanced on doping with CCl_4 and its reassignment²⁴ to ScO^+ is supported. Unfortunately, the ScN^+ species, calculated 22 cm^{-1} above ScN , could not be observed here.

$\text{M} + (\text{NO})_2$. Upon annealing, the marked growth of the bands at 1863.2 and 1776.1 cm^{-1} at the expense of the strong band at 1871.7 cm^{-1} in the $\text{M} + ^{14}\text{N}^{16}\text{O}$ experiments is indicative of dimerization of the NO molecule. As the matrix is annealed and nitric oxide dimerizes, the importance of monomer chemistry begins to decline because of the shrinking population of NO in the system. At the same time, the chemistry of $(\text{NO})_2$ is expected to become much more prevalent and the reaction products of $(\text{NO})_2$ with the diffusing transition metal atoms must be considered. In the experiments with Ti several bands appear on matrix annealing and can be associated with metal reactions with $(\text{NO})_2$.

The band growing in on annealing at 1581.3 cm^{-1} with Ti and NO shifts to 1552.9 with ^{15}NO (ratio 1.018 29) and exhibits a triplet absorption with the isotopic mixture. This denotes the vibration of two equivalent NO subgroups. The 1552.9 cm^{-1} band shifts to 1510.7 cm^{-1} with $^{15}\text{N}^{18}\text{O}$ (ratio 1.027 93), which is appropriate for a nitrosyl vibration, and the product is thus identified as $\text{Ti}-(\eta^1\text{-NO})_2$. Calculations at the DFT level predict an extremely strong antisymmetric N–O stretching mode at 1590.0 cm^{-1} for this dinitrosyl complex.

A weak 1125.1 cm^{-1} band appeared on first annealing, diminished on photolysis, and increased even more on final annealing. This band shifted with ^{15}NO (ratio 1.018 56) and $^{15}\text{N}^{18}\text{O}$ (ratio 1.026 21) and gave triplets with both isotopic mixtures, which indicate two equivalent NO subunits. The side, side-bound dimer $\text{Ti}-(\eta^2\text{-NO})_2$ is calculated by DFT to strongly absorb at 1144.2 cm^{-1} , and the 1125.1 cm^{-1} band is assigned accordingly.

The bands at 1488.5 , 1208.8 , and 977.1 cm^{-1} (Table 2) all share similar annealing and photolysis behavior and can therefore be associated with vibrations of the same molecular species. These bands are very weak or unobserved on deposition but grow in markedly on warming the matrix, reaching their maximum intensity upon the highest temperature annealings. In addition, the species giving rise to these bands also shows significant photosensitivity as indicated by the disappearance of all three bands on broad-band photolysis. Such drastic photolytic behavior makes assigning these three bands to the same species straightforward. In addition, similar absorptions have been observed in experiments with Zr and Hf.³⁰ In the reactions with a $^{14}\text{N}^{16}\text{O}/^{15}\text{N}^{16}\text{O}$ mixture, the highest and middle frequency bands of each set split into a quartet (Table 2), indicating that both of these vibrations arise from the motions of two symmetry inequivalent nitrogen atoms. The relatively large $^{14}\text{N}/^{15}\text{N}$ isotope ratios exhibited by these modes also indicate that these are primarily N–N stretching coordinates ($1488.8/1448.7 = 1.027\ 47$ and $1208.8/1178.8 = 1.025\ 45$). In addition to the large nitrogen isotopic shift, there is a distinct oxygen isotopic dependence, as evidenced by the doublet structure in the mixed $^{15}\text{N}^{16}\text{O}/^{15}\text{N}^{18}\text{O}$ experiments. These isotope

splittings provide evidence for a molecular subunit of the stoichiometry NNO. It is also interesting to note that since the frequencies of these bands are relatively invariant among the Ti, Zr, and Hf experiments, it is reasonable to believe that the chromophore giving rise to these absorptions is relatively robust, which is consistent with a coordinated nitrous oxide molecule. DFT calculations of isotopic frequencies (Table 5) provide a very good match for these unique observed isotopic ratios and show that this Ti + (NO)₂ reaction product is OTi(N₂)O.

The bands at 2294.2, 960.6, and 909.3 cm⁻¹ provide evidence for other Ti + (NO)₂ reaction products. The 2294.2 cm⁻¹ band has characteristic N₂O isotope shifts and suggests an (NNO)-(TiO) complex, and the 960.6 cm⁻¹ band exhibits the diatomic TiO shift and is appropriate for this mode in the latter complex. The 909.3 cm⁻¹ band gives the TiO₂ oxygen-18 shift and the 1/2/1 triplet mixed isotopic pattern for two equivalent oxygen atoms. Therefore, the most stable (N₂)(TiO₂) complex is proposed, in agreement with earlier reactions of Ti, O₂, and N₂.³¹ The formation of TiO₂ in these experiments suggests the possible use of titanium for the removal of NO from auto exhausts.

The 1633.2 and 1067.1 cm⁻¹ bands in Sc + NO experiments increase steadily on the annealing sequence, reaching maximum intensity on the final annealing. No absorptions in either region give triplet isotopic patterns for two equivalent NO subgroups, in contrast to the Ti system. The 1067.1 cm⁻¹ band shifts to 1056.7 cm⁻¹ (ratio 1.00984) and to 1022.1 cm⁻¹ with ¹⁵N¹⁸O (ratio 1.03383) and the bands broaden in the mixed isotopic experiments, providing evidence for a small secondary isotope effect. DFT calculations predict strong absorptions at 1642.7 cm⁻¹ (488 km/mol) and 1076.7 cm⁻¹ (290 km/mol) for the Sc-(η^1 -NO)-(η^2 -NO) complex, i.e., end- and side-bonded, [NO]-ScNO, which are in agreement with the above absorptions.

Other Absorptions. There remain absorptions that appear on annealing and are thus due to combinations of reagents and primary reaction products. The most perplexing is the 1192 cm⁻¹ band with Sc, which shows a 1.037 16 isotopic ratio for 14/15 (in excess of the pure N-N value) and doublets with isotopic mixtures. This secondary product species displays an unusual vibrational interaction and cannot be identified here. The 792.5 cm⁻¹ band with Sc is produced on photolysis, exhibits the 14/15 ratio 1.020 74, and has doublets with isotopic mixtures. This band may involve the ScN product of reaction 2c in combination with NO, but this species cannot be characterized.

Conclusions

Laser-ablated Sc and Ti atoms react with NO during condensation in excess argon. Matrix infrared spectra show that the major products are the side-bonded Sc[NO] species and the inserted NScO and NTiO molecules on the basis of isotopic substitution (¹⁵N¹⁶O and ¹⁵N¹⁸O) and DFT calculations of isotopic frequencies, which provide a match for two modes in three isotopic modifications for each molecule. The NScO and NTiO molecules are nitride/oxides with M-O modes only 46–88 cm⁻¹ below diatomic metal oxides but M-N modes 314–442 cm⁻¹ lower than the diatomic metal nitride molecules. Evidence is also presented for the nitrosyls ScNO and TiNO, the Sc[NO]⁺ cation, and the NTiO⁻ anion. Titanium is particularly reactive with (NO)₂, and this metal may be useful in the catalytic removal of NO from auto exhausts.

The agreement between observed and calculated frequencies using the BP86 functional for these small Sc- and Ti-containing species is remarkable. This agreement is not only in position of the calculated frequencies (scale factors: NScO 0.995, 1.026; Sc[NO] 0.978, 1.004; NTiO 0.962, 0.944; which are in the range of literature values³²) but also in the normal vibrational modes as measured by isotopic frequency ratios and shifts and by relative band intensities.

Acknowledgment. We gratefully acknowledge support for this research from the National Science Foundation and the Air Force Office of Scientific Research.

References and Notes

- (1) Cotton, F. A.; Wilkinson, G. *Advanced Inorganic Chemistry: A Comprehensive Text*, 5th ed.; Interscience Publishers: New York, 1988.
- (2) Yamamoto, A. *Organotransition Metal Chemistry: Fundamental Concepts and Applications*; Wiley-Interscience: New York, 1986.
- (3) Drago, R. S., *Physical Methods for Chemists*, 2nd ed.; Saunders College Publishing: Philadelphia, 1992.
- (4) Stryer, L. *Biochemistry*, 4th ed.; W. H. Freeman Publishers: New York, 1995.
- (5) Wink, D. A.; Grisham, M. B.; Mitchell, J. B.; Ford, P. C. *Methods in Enzymology*; Academic Press: San Diego, 1996.
- (6) Ward, T. R.; Alemany, P.; Hoffmann, R. *J. Phys. Chem.* **1993**, *97*, 7691.
- (7) Zhou, M. F.; Andrews, L. *J. Phys. Chem. A* **1999**, *103*, 478.
- (8) Zhou, M. F.; Andrews, L. *J. Phys. Chem. A* **1998**, *102*, 7452.
- (9) Burkholder, T. R.; Andrews, L. *J. Chem. Phys.* **1991**, *95*, 8697.
- (10) Hassanzadeh, P.; Andrews, L. *J. Phys. Chem.* **1992**, *96*, 9177.
- (11) Frisch, M. J.; Trucks, G. W.; Schlegel, H. B.; Gill, P. M. W.; Johnson, B. G.; Robb, M. A.; Cheeseman, J. R.; Keith, T.; Petersson, G. A.; Montgomery, J. A.; Raghavachari, K.; Al-Laham, M. A.; Zakrzewski, V. G.; Ortiz, J. V.; Foresman, J. B.; Cioslowski, J.; Stefanov, B. B.; Nanayakkara, A.; Challacombe, M.; Peng, C. Y.; Ayala, P. Y.; Chen, W.; Wong, M. W.; Andres, J. L.; Replogle, E. S.; Gomperts, R.; Martin, R. L.; Fox, D. J.; Binkley, J. S.; Defrees, D. J.; Baker, J.; Stewart, J. P.; Head-Gordon, M.; Gonzalez, C.; Pople, J. A. *Gaussian 94, Revision B.1.*; Gaussian, Inc.: Pittsburgh, PA, 1995.
- (12) Becke, A. D. *Phys. Rev. A* **1988**, *38*, 3098. Perdew, J. P. *Phys. Rev. B* **1986**, *33*, 8822.
- (13) Chertihin, G. V.; Andrews, L.; Rosi, M.; Bauschlicher, C. W., Jr. *J. Phys. Chem. A* **1997**, *101*, 9085. The 976.3 cm⁻¹ band is due to ScO⁺.
- (14) Chertihin, G. V.; Andrews, L.; Bauschlicher, C. W., Jr. *J. Am. Chem. Soc.* **1998**, *120*, 3205.
- (15) Frisch, M. J.; Pople, J. A.; Binkley, J. S. *J. Chem. Phys.* **1984**, *80*, 3265 and references therein.
- (16) Wachters, A. J. H. *J. Chem. Phys.* **1970**, *52*, 1033.
- (17) Hay, P. J. *J. Chem. Phys.* **1977**, *66*, 4377.
- (18) Chertihin, G. V.; Andrews, L. *J. Phys. Chem.* **1995**, *99*, 6356.
- (19) Kushto, G. P.; Souter, P. F.; Chertihin, G. V.; Andrews, L. Submitted for publication (Ti + N₂).
- (20) Andrews, L.; Zhou, M. F.; Willson, S. P.; Kushto, G. P.; Snis, A.; Panas, I. *J. Chem. Phys.* **1998**, *109*, 177 and references therein.
- (21) Illenberger, E. *Ber. Bunsen-Ges. Phys. Chem.* **1982**, *86*, 252. Matejcek, S.; Kiendler, A.; Stamatovic, A.; Märk, T. D. *Int. J. Mass. Spectrom. Ion Processes* **1995**, *149/150*, 311.
- (22) Prochaska, F. T.; Andrews, L. *J. Chem. Phys.* **1977**, *67*, 1091 and references therein.
- (23) Maier, G.; Reisenauer, H. P.; Hu, J.; Hess, B. A., Jr.; Schaad, L. J. *Tetrahedron Lett.* **1989**, *30*, 4105.
- (24) Zhou, M. F.; Andrews, L.; Bauschlicher, C. W., Jr.; Roos, B. O.; Tobias Johnson, J. R.; Panas, I.; Snis, A. To be submitted for publication (ScO₂⁻).
- (25) Thiem, T. L.; Salter, R. H.; Gardner, J. A. *Chem. Phys. Lett.* **1994**, *218*, 309.
- (26) Thomas, J. C.; Bauschlicher, C. W., Jr.; Hall, M. B. *J. Phys. Chem. A* **1997**, *101*, 8530.
- (27) Blanchet, C.; Duarte, H. A.; Salahub, D. R. *J. Chem. Phys.* **1997**, *106*, 8778.
- (28) Rosi, M.; Bauschlicher, C. W., Jr.; Chertihin, G. V.; Andrews, L. *Theor. Chem. Acct.* **1998**, *106*, 99.
- (29) Zhou, M. F.; Andrews, L. *J. Am. Chem. Soc.* **1998**, *120*, 13230.
- (30) Kushto, G. P.; Andrews, L., To be submitted for publication (Zr, Hf, Th + NO).
- (31) Chertihin, G. V.; Andrews, L. *J. Phys. Chem.* **1994**, *98*, 5891.
- (32) Scott, A. P.; Radom, L. *J. Phys. Chem.* **1996**, *100*, 16502.